Journal of Harbin Engineering University
ISSN: 1006-7043
Vol 44 No. 11
November 2023

Solar Powered Cardiac Pacemaker with Skin Equivalent Circuit

T. Suganya [1*], V. Rajendran[2], P. Mangaiyarkarasi[3]
[1*]Research Scholar, Department of Electronics and Instrumentation Engineering, Annamalai University, Tamil Nadu, India
[2]Principal, Government Polytechnic College for Women, Coimbatore, Tamil Nadu, India
[3]Associate Professor, Department of Electronics and Instrumentation Engineering, Annamalai University, Tamil Nadu, India

Abstract
Medical electronic implants can basically work on the well-being and personal satisfaction of individuals. These implants are usually fueled by batteries, which have a limited lifespan and as a result need to be replaced occasionally using surgery. In the batteries, subcutaneous sun-based cells, which can generate energy by retaining the light transmitted through the skin, have been proposed as an economic force to control medical electronic insertions in the body. This paper is to develop a Maximum Power Point Tracking (MPPT) controller for an equivalent skin model with battery-less cardiac pacemaker. In the proposed methodology, equivalent skin model with battery-less cardiac pacemaker is implemented by varying the electrical parameters such as resistance and capacitance of epidermis, dermis and subcutaneous layer (R_{sc}, C_{sc} and R_s). The Photovoltaic cell is utilized to power the cardiac pacemaker to design a battery-less cardiac pacemaker. To manage environmental conditions, an efficient Maximum Power Point Tracking (MPPT) controller is designed in the implantable cardiac pacemaker. In the MPPT controller, the Fractional Order Proportional Integral Derivative (FOPID) is designed which can be utilized to extract the maximum power from the PV system. In the FOPID controller, Chimp Optimization Algorithm (COA) is utilized to empower the FOPID controller performance. The proposed methodology is implemented in MATLAB/Simulink platform and it is evaluated by the output voltage, output current and output power. The proposed methodology is compared with the conventional methods such as Particle Swarm Optimization (PSO) and Grey Wolf Optimization (GWO) respectively.
Keywords: Battery-free Cardiac Pacemaker, Chimp Optimization Algorithm, DC-DC converter, Photovoltaic Cell, Skin Equivalent Model, Epidermis, Dermis And Subcutaneous layer, Resistance, Capacitance, Implantable Cardiac Pacemaker, Maximum Power Point Tracking and Battery.

1. Introduction

The energy coming from the climate would be an attractive substitute for giving medical inserts the ability to maintain. The sustainable energy sources are an attractive solution to provide essential power to the cardiac pacemaker. In recent years, the solar energy is utilized to power the cardiac pacemaker [1] that can be embedded into implantable microelectronic clinical gadgets. Light is penetrable and less intuitive with natural tissues. Its dependence on frequency allows it to control a specific area somewhere within the tissue. A spectacular study area that meets the needs of the classification of heart patients is the applicable cardiac biosensor. Despite the fact that sophisticated batteries used for embedded heart pacemakers are used for longevity and high storage capacity [2], regular patient batteries should be replaced within 8-10 years of pacemakers being fitted. Implementing compatible medical gadgets depends on, for example, compatible cardiac biosensors, practical electricity [3]. The availability of batteries for compatible cardiac pacemakers is a significant requirement, the trade of which creates suffering for patients despite high cash transactions.

It is, however, a primary test of power collection in such compatible gadgets. Most compatible gadgets are controlled exclusively using batteries, which require careful replacement as possible [6]. Part of the limitations of these gadgets is their size, longevity and the risk that the batteries may release harmful substances [7]. Following that, efforts to reduce the size of the gadgets should reduce the weight and size of these gadgets. Due to the limited battery limit, transformers are

forced towards produce power from the human body or include an atmosphere that extends battery life [8]. There are various approaches to extracting energy from the subsoil using bio fuel cells (BC), thermal electric generators (TEGs), piezoelectric generators (PEGs), radio frequency (RF) harvesters and photovoltaic (PV) cells and Energy Harvesting Strategies [9]. Unfortunately, a significant number of these practices have constraints due to their enormous size, low yield power thickness or powerless energy yield. In conjunction with the previously mentioned approaches, compatible PV cell inventions convert large amounts of energy from the sun into effective electrical energy [10].

The specific idea of PV cells is to utilize, organize and stack them with the adaptability to meet the yield power and voltage of an implantable application. In addition, advanced strategies for working with the productivity of this innovation using light caching methods, MPPT and other power management practices are proposed in writing. Accordingly, various MPPT techniques have been used to accurately diagnose MPP [12]. These ratings are represented by various points such as complexity, cost, required sensor type, implementation and immovable quality of these MPPT estimates, Perth and Observation (P&O) calculations are the most commonly used because they are easier to implement and less problematic [13]. Nevertheless, now again as a fast-paced environment type, regular P&O calculation gets stuck after MPP. To manage this problem, various improvements in the normal P&O rating have been used to implement more intense power P.V. The design is available in a wide range of MPPT controllers including PV.

Main contribution and organization of the paper

The main contribution of the paper is as follows,

- This paper is to develop a MPPT controller in battery-less cardiac pacemaker. In the proposed methodology, an equivalent skin model with battery-less cardiac pacemaker is designed.
- The Photovoltaic cell can be utilized to power the cardiac pacemaker through equivalent skin model.
- The PV may be affected due to environmental conditions which will be solved by the MPPT controller.
- The proposed battery-less cardiac pacemaker implemented using MATLAB and the performance is evaluated in terms of maximum power, maximum voltage, maximum current, irradiance, the input power of pacemaker, and output power of pacemaker.
- The proposed methodology is contrasted with existing techniques like PSO and GWO based optimized pacemaker.

The paper is organized as follows; section 2 provides the review of previous published paper related with the design of implantable cardiac pacemaker. Section 3 delivers the detail description of the projected methodology with the skin equivalent model and Section 4 analyses the outcomes of the projected methodology. The summary of the article is presented in section 5.

2. Literature Review

Various methods are developed by researchers for tracking MPPT from the PV system. Some of the methods are reviewed in this section.

Munna Khan et al., [16] have introduced low-power solar power supply for battery-powered cardiovascular biosensors. The primary focus of this paper is to generate power from a PV display placed under the skin to recharge the depleted battery of compatible cardiac biosensors. The new philosophy is that the embedded PV removes the greatest amount of energy from receiving Near-Infrared (NIR)light through the skin from the outside and depends entirely on the power provided by the embedded PV cluster for its operation. The program uses a voltage-based MPPT technique that uses virtual open-circuit voltage to manage cargo continuously. The activation uses a PV cluster proven in SPICE, which provides a capacity of 10-25 mW for a 6-14 mA current purpose. Reproductions show that the fitting reserve generates enough power and voltage to charge the battery of low-power compatible cardiac biosensors such as the pacemaker.

Andreas Haeberlinet al., [17] have introduced three attempts to deal with the possibility of daytime controlled heart rate. First, the harvestable power was estimated. Assuming, the submersible embedded 1 cm2 sun-based module can collect 5002500 W from daylight (3 mm

implant depth). Then, ex vivo estimates were made by sun-based cells under a solar-powered test system and pig skin folds provided for actual daylight. Ex vivo ratings under actual daylight came with an average resolution of 4941W/cm2 [intermediate range (IQR) 3767-5598 W / cm2, medium skin fold thickness 3.0 mm (IQR 2.7-3.3 mm)]. The effect force was firmly dependent on the implant depth (peSpearman = 00.86, P <0.001). For a long time, the battery-less single-chamber pacemaker, controlled by a 3.24 cm2 solar-based module, was embedded in the Vivo mainly for measuring yield energy and increasing speed.

M.V. Thollet al.,[18] has introduced a customizable model for measuring the power output of a subterranean solar energy reaper for electronic inserts. Sub thermal energy ripening can be used for a wide range of applications and is not limited to heart rate. Different applications can incorporate embedded sensors that more accurately measure blood flow strain or increase sensor speed to detect falls or accidents in the elderly. The Monte Carlo theory, introduced, allows estimating the energy yield of a subterranean solar cell for different opening times, implant depth, skin types and cell sizes. This reproduction revealed the need to create extraordinary sunlight-based cells for enhanced intimate infrared radiation, to control the specific light time specified for the useful material of the sub thermal sun-based collection for medical energy gadgets for all skin types.

Lin Dong et al.,[19] introduced project standards for cardiac energy reapers and sensors. In addition, delayed improvements in cardiovascular energy harvesting and detection of gadgets in both Vivo and in vitro were observed and studied. In view of the piezoelectric and triboelectric schemes such supportable energy systems provide a promising way to reduce the reliance on batteries to drive cardiovascular gadgets and other implantable biomedical devices (IMDs).

Adrian Jurbusenet al., [20] have introduced the swiss method of heart-powered lead and battery-less pacemakers. Gathering energy from the cardiac output can take two significant controls of the current pacemaker. This study revealed the practicality of lead and battery low speed control using the heart's own mechanical motion. Dynamic clinical insertions play an important role in cardiac medicine. Their job is to diagnose and treat patients with unintended side effects. Moreover, they have relied on working independently for a long time. Nevertheless, the most well-known electrical plugs, the remaining electrical plugs in the heart pacemakers run on an internal battery, which must be replaced before the end of its lifespan.

3. Proposed System Model

The proposed structure is containing of a Photovoltaic cell, optimized MPPT controller, boost converter and skin equivalent circuit model. This structure is mainly developed to power the cardiac pacemaker without any interruption which illustrated in figure 1. The full embedded set-up is available near the infrared from the laser diode and the focal point function placed on the outside of the human body. Near-infrared enters well into human skin in addition can no longer be used instead of PV array, which is constantly inaccessible and has low penetration power. In this way, for a similar episode of radiation on human skin, the PV system provides additional power from nearby infrared radiation when contrasted with daylight radiation. Furthermore, Near-Infrareds are less destructive to human skin than conventional radiation. Accordingly, a minor PV array is producing more power using nearby infrared radiation than daytime radiation aimed at a currently compatible cardiac pacemaker, which requires the power of demand for µW to continue the rhythmic function of the heart.

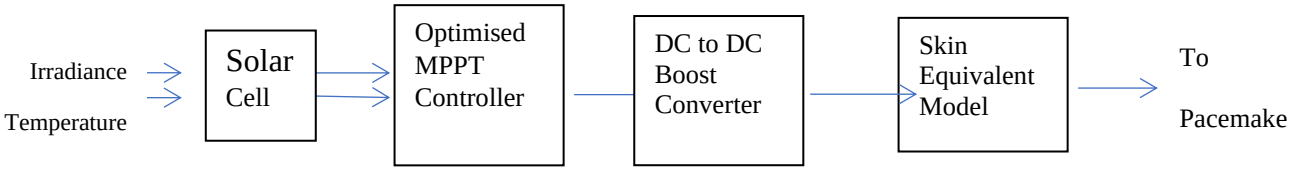

Figure 1: Model of the proposed system

The Main Objective Of The Projected Technique Is To Develop A Battery-Free Cardiac Pacemaker With The Help Of A PV And MPPT Controller For Skin Equivalent. The Proposed Controller Is Utilized To Manage The Cardiac Pacemaker Functions. The MPPT Controller Is Designed With A Fractional-Order Proportional-Integral-Derivative (FOPID) Controller Utilized To Manage The Monitoring The Operation Of Cardiac Pacemakers.

3.1. Skin Equivalent Model

The Skin Equivalent Model Is Needed For Electrical Implementation Because Of The Immeasurable Impedance Of It. Skin Equivalent Circuit Is Developed By RC Equivalent Circuit. The Values Are Given As Follows: Rsc=1kω To 5000kω, Csc=10nf To 100nf, Rs =1Ω To 1 Kω , Where Rsc Is Resistance Of Epidermis Layer , Csc Is Capacitance Of Epidermis Layer And Rs Is Resistance Of Dermis And Subcutaneous Layer . Resistance RSC And A Dielectric Capacitance CSC Are Placed In Parallel Combination To Represent The Resistive Property And Capacitive Property Respectively. This Parallel Combination Is Placed In Series With A Small Resistance RS Which Constitute The Resistance Offered By The Dermis And Subcutaneous Layer Which Are Deep Layers Of Skin. The Equivalent Circuit Model Is Presented In The Figure 2.

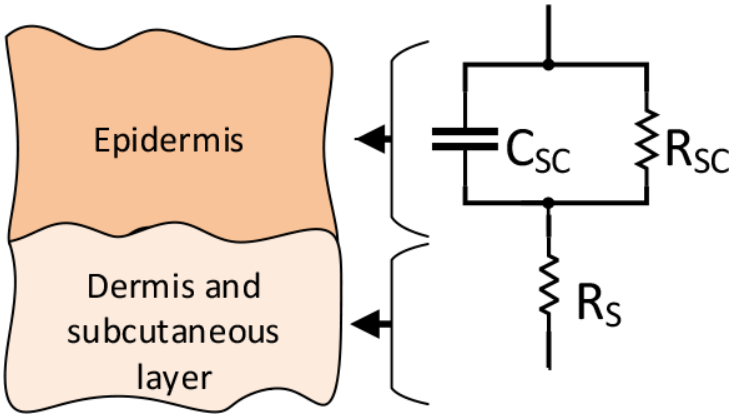

Figure 2: Skin Equivalent Circuit Model

3.2. Modelling of PV system

In this section, a normal mathematical formulation of the PV cell is given. The PV cells can be measured as electrical devices which generate electrical power from sunlight energy based on irradiance level. The sunlight energy is collected with the presentation of a PV panel which is named as sustainable energy source. The PV panel can be designed with the consumption of a semiconductor panel which absorbs photons of sunlight energy and omits the electrons which all taken number of atoms based on behavior potential difference can be produced [21]. Associated with atom characteristics, current flow can be processed and electricity generated which is utilized in many different applications. The MPPT controller must be designed towards excerpt the highest power from PV through avoiding problems in environmental behavior. The general design of the PV system can be presented in figure 3. The parallel resistor, photocurrent, diode with equivalent circuit model are designed which provides leakage current and internal resistance encourage the current flow in PV panel.

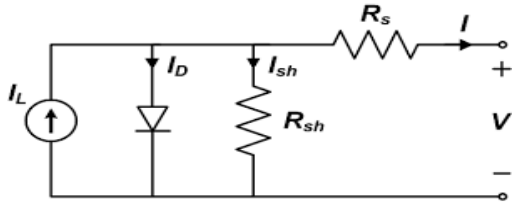

Figure 3: Equivalent circuit model of PV system

The current in addition voltage of a solar cell is formulated as the following,

$$I_c^{PV} = \frac{I_{ph}}{1 - C^{-d}}\left[\exp^{\frac{V_{oc}}{a}}\left(\frac{qV + qr_vI}{NKT}\right) - 1\right] - \frac{V + R_sI}{R_{sh}} \qquad (1)$$

Where,

I_{ph} can be described as is the electric current of PV

I can be defined as a current of PV panel

$q = \left(1.6 * 10^{-19} C\right)$ can be considered as electron charge,

T can be considered as the temperature of each cell in the PV panel,

N can be defined as an ideal factor of PV

R_{sh} can be described as shunt resistance

R_s can be described as series resistance

V_{oc} can be described as open-circuit voltage

α can be described as temperature coefficient of short circuit current under standard test conditions

K can be described as Boltzmann's constant

C can be described as temperature coefficient

r_v can be described as module parallel resistance

V can be described as diode thermal voltage

Based on the irradiance (Temperature) changes, the PV panels can be developed in addition controllers. In each solar panel, the various irradiance levels are considered for generating power. The solar panel output power is changed because of irradiance level changes. The proper control signals generation is maintained in the constant irradiance with the DC-DC converter. In the MPPT controller, the maximum power is attained with the assistance of the PID controller. Sometimes, the environmental conditions may be affecting the generated power. For this reason, MPPT is developed to manage the different weather conditions. In the proposed MPPT controller, the error power is computed which is corrected by providing the optimal pulses to the DC-DC boost converter. The optimal pulses are calculated related on the FOPID controller. In the FOPID controller, the optimal pulses are selected with the help of the optimization algorithm used.

3.3. FOPID controller

In the proposed controller, the FOPID controller can be used to reduce the error of different parameters of PV power. Based on the differentiation and connection of non-integer order, the fractional-order controller may work with fractional-order differential equations. In general, PID system has three different control parameters, such as proportional and derivative controllers. In the proposed controller, the FOPID controller can be used to reduce the error of different parameters of PV power. Based on the differentiation and connection of non-integer order, the fractional-order controller may work with fractional-order differential equations. The general PID system has three different control parameters, such as proportional and derivative controllers. The PID operation performance may be improved with the consumption of adding two parameters and form a FOPID controller which increases two control parameters. The FOPID controller may be mathematically presented as follows. The main variation among the PID controller in addition FOPID controller can be, FOPID [22] controller has extra two control parameters and the derivation order are not an integer value. This behavior given additional degrees of liberty for tuning the controller which encourages the best dynamic parameters with contrasted conventional PID controller. In recent years, compared with the PID controller, the FOPID controller has the best performance of controlling error values of the micro grid system.

The FOPID controller output is mathematically formulated and presented as follows,

$$U(t) = K_p E(t) + K_I D_t^{-\lambda} E(t) + K_d D_t^{-\mu} E(t) \quad (2)$$

$$E(t) = \Delta P_{tie}(t) + B_i \Delta \omega_i(t) \quad (3)$$

The transfer function of the FOPID controller can be presented below,

$$G(s) = K_p + \frac{K_i}{S^{\lambda}} + K_d S^{\mu} \quad (4)$$

The reference value is compared with the present value of PV power to compute error values which is denoted by $E(t)$ and the control signal of the system is mentioned as$U(t)$. The FOPID controller parameters have five parameters that provide the best results to enhance the presentation of the structure. Various PID regulator range adjustment procedures are used for decentralized power framework load recurrence regulators. It is about the idea of boundary spacing to control common operating system improvements such as COA calculation. In the light of thinking using genetic directors, the computational unpredictability of this general population-based estimate has been extended [23]. Direct viewing is appropriate for exposing and recognizing abnormal organisms, which are no longer used as progress estimates as part of the ongoing operation of a power microgrid structure. In this paper, the COA calculation is proposed to control the MPPT of the PV structure.

3.3. Chimp Optimization Algorithm

In this proposed methodology, COA is utilized to select the optimal gain parameters of the FOPID controller. The mathematical formulation of COA is presented as follows,

3.3.1. Inspiration

Normally, the fission-fusion society is a chimp's society. This is considered as one of the societies, the combination of society may be a time-variant function. Additionally, in society, each member has a specific duty and special ability that may change over time. From the consideration, the aim of independent concepts is developed in this algorithm. Hence, every group of chimpanzees separately attempts to find the search space with its singular characteristics intended aimed at specific duty. Generally, four types of chimps are presented such as attackers, chasers, barriers, and drivers. Based on these types, the behaviors of the chimps in the hunting process are changed for efficient hunt operation. In the chimp's algorithm, the drivers have collected the prey without doing the hunting process. Barriers residence themselves in plants to create a dam crossway the leakage route of the prey [24]. The prey is grabbed by chasers rapidly. At last, the attackers are identifying the escape route of the prey down into the inferior canopy. Attackers are required to have more efficient in identifying the proceeding change of prey. Moreover, the attackers have been collected with the meat larger piece after an efficient hunt.

In Chimp calculation, the attack method is strictly related to actual ability, intelligence, and age. Also, Sims can change practices during a particular chase or interact with their strategy as a whole. It is authorized by the chimps Chase to execute meat in exchange for social honors such as preparation and firm assistance. Henceforth, by opening another domain of interest and benefits. chimp may indirectly affect the chase. People use social motivation as chimps. In this way, the chimps have an advantage compared to other social predators. In addition to sexual motivation, start the sims to act turbulent as the last advance of the chase. Therefore, bulk chips drop the mistakes of obtaining meat independently. From the thinking of the social behavior of the Sims, it can be isolated into two primary stages, such as investigation and misuse. There is a way to track, prevent and drive prey in the investigation. Misuse is considered a prey attack. Details of misuse and investigation numbers are introduced as follows,

3.3.2. Driving and chasing the prey

In the COA, the prey can be hunted throughout the exploitation also exploration stages. The mathematical design of chasing also driving prey is formulated as follows,

$$D = \left| c.x^{prey}(T) - M.x^{chimp}(T) \right| \quad (5)$$

$$x^{chimp}(T+1) = x^{prey}(T) - A.D \quad (6)$$

Where, x^{prey}, x^{chimp} can be described as position vector of chimp and prey, T can be described as a

number of current iterations, and $A, M\ and\ C$ can be described as coefficient vectors. The position vectors of the COA is computed based on the below equation,

$$A = 2.F.R^1 - a \quad (7)$$
$$C = 2.R^2 \quad (8)$$
$$M = Chaotic\ Value \quad (9)$$

Where, R^1 and R^2 can be described as random parameters which in the variety of [0,1], F can be described as coefficient which decreased non-linearly from 2.5 to 0 by the iteration procedure (in both explorations also exploitation). M can be described as a chaotic parameter computed based on different chaotic maps. Hence, the vector describes the behaviour of sexual incentive of chimps in shooting behaviour.

Exploration phase

The attack behaviour of the chimp's mathematical model is designed as follows, firstly, the chimps can provide the location of the prey, and secondly, they can orbit it. Finally, predators are generally maintained by attackers. The chaser, barrier, and driver are usually involved in the hunt. At the research stage, there was no information about the optimal condition of the prey during the initial repetition. This state of the chaser, block and drive must be updated using the attacker's status. So, four optimal solutions can be saved and the other chimps are stopped to update the positions related to the locations of the best chimps. This creation is presented mathematically as follows,

$$d^{Attacker} = |C^1 X^{attacker} - M^1 D| \quad (10)$$
$$d^{Barrier} = \left|C^2 X^{barrier} - M^2 X\right| \quad (11)$$
$$d^{Chaser} = |C^3 X^{Chaser} - M^3 X| \quad (12)$$
$$d^{Driver} = \left|C^4 X^{driver} - M^4 X\right| \quad (13)$$
$$X^1 = X^{Attacker} - A^1(d^{Attacker}) \quad (14)$$
$$X^2 = X^{Barrier} - A^2(d^{Barrier}) \quad (15)$$
$$X^3 = X^{Chaser} - A^3(d^{Chaser}) \quad (16)$$
$$X^4 = X^{Driver} - A^4(d^{Driver}) \quad (17)$$
$$X(T+1) = \frac{X^1 + X^2 + X^3 + X^4}{4} \quad (18)$$

The search agent position is updated in the search space based on another chimp position. so, the chimp's final position is arbitrarily placed in the orbit which is described as drivers, chasers, barrier, and attacker positions.

Exploitation phase

As beforehand mentioned, the chimps will hunt the victim by attacking process while the prey stops running. In the attacking process of chimps, the value of f is linearly minimized. The vector of a also reduced in the manner of f vector. Additionally, the a is an arbitrary variable in the interval of $[-2f, 2f]$. Additionally, COA chasing [25], blocking, and driving mechanisms have reinforced exploration capability and it may still be at the risk of local minima trapping conditions. Hence, the exploration is a required portion to achieve the best results. In COA, chimps deviate to attack the prey and converge to attack the prey. The vector a is located to mathematical design this characteristic so that inequality parameters. To avoid local optima entrapment, the chimps forced to diverge from prey which formulated as $|a| > 1$. To achieve global optima, the chimps forced to converge at prey location which formulated as$|a| < 1$.

Exploitation phase using the social incentive

In the COA, the social incentive and society of chimps which related to meat hunting. In the final stage of the chimp hunting process, the chimp may abort its hunting process. Hence, they chaotically attempt to grab hunting meat for social essences. These characteristics of the chaotic map are designed with chaotic maps which formulated as follows,

$$X^{chimp}(T+1) = \begin{cases} x^{prey}(t) - A.D & if \quad \mu < 0.5 \\ Chaotic\ value & if \quad \mu > 0.5 \end{cases} \quad (19)$$

Where μ can be described as an arbitrary number in the interval of [0,1]. Initially, they generate a random population of chimps. Secondly, all chimps are arbitrarily divided by different groups such as

driver, chaser, barrier, also attacker. After that, every chimp position updates the f coefficients with the consideration of the own group method. The optimal prey location is identified in the iteration based on driver, chaser, barrier, and attacker. Then the distance from the prey, the positions are updated. Additionally, the optimal tuning of the m and c, the fast convergence rate and faster. Additionally, the value of f can be adjusted from 2.5 to 0 which empowers the process of exploitation. Finally, the condition of the divergence and iterations are checked which provides the optimal results to manage the results. With the help of COA, the optimal gain parameter is selected. After that, the proposed classifier is utilized to classify breast cancer from mammogram images.

4. Results and Discussion

The presentation of the solar-powered cardiac pacemaker can be validated and justified in this section. The solar-powered cardiac pacemaker with FOPID – COA is implemented using MATLAB.

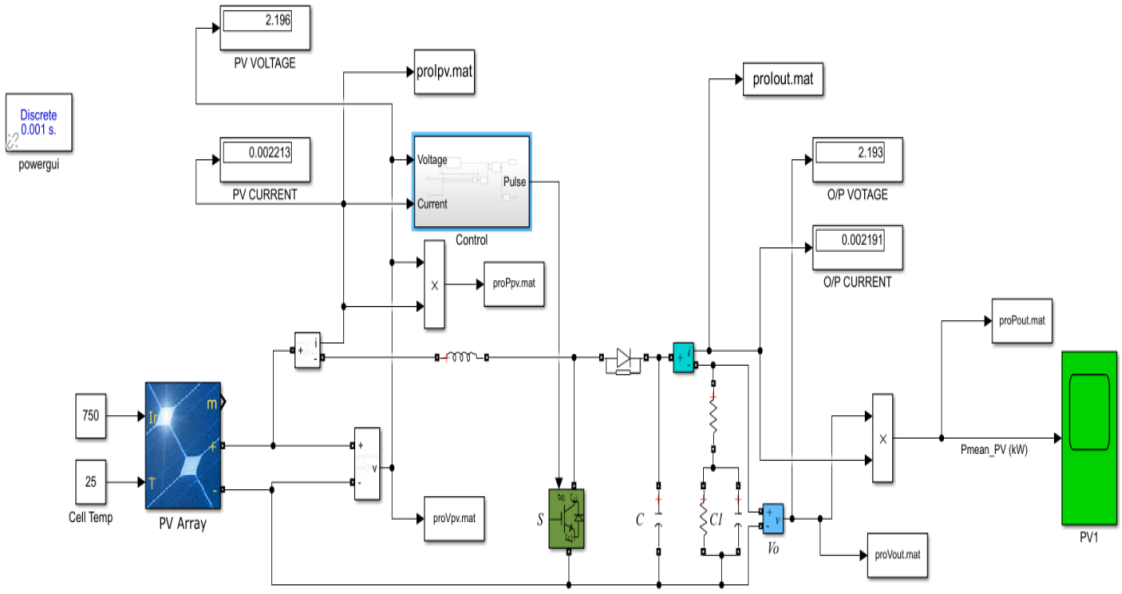

Figure 4. Proposed simulink diagram

Table 1: Parameters of the Proposed Technique

S. No	Description	Parameters
1	Series resistance	0.0005 ohm
2	Shunt resistance	10000.005 ohms
3	Diode ideality factor	2.999
4	Diode saturation current	1.5749e^15 A
5	Light generated current	0.0080306 A
6	Cells per module	1
7	Short circuit current	0.008 A
8	Current at maximum power point	0.007 A

9	Temperature coefficient	0.061745^0C
10	Voltage at maximum power point	5V
11	Open circuit voltage	6V
12	Maximum power	0.035W

O/P value for various Skin Equivalent values and their corresponding voltage and current output values are tabulated in Table 2. The proposed methodology generates stable output for each iteration.

Table 2: Simulation results for various skin equivalent values

Rsc = 1000 Ohm; Csc = 10 nF									
Rs	OP V	OP I	OPPower COA	OP V	OP I	OPPower PSO	OP V	OP I	OPPower GWO
1	2.193	0.002191	0.0048	2.189	0.00218	0.0048	2.178	0.00216	0.0047
50	2.195	0.002091	0.0046	2.191	0.00207	0.0045	2.188	0.00205	0.0045
100	2.197	0.001997	0.0044	2.193	0.00198	0.0043	2.19	0.00195	0.0043
250	2.202	0.001761	0.0039	2.196	0.00166	0.0036	2.194	0.00159	0.0035
500	2.207	0.001471	0.0032	2.199	0.00142	0.0031	2.198	0.00138	0.0030
750	2.211	0.001263	0.0028	2.203	0.0012	0.0026	2.203	0.00119	0.0026
1000	2.213	0.001107	0.0024	2.206	0.00107	0.0024	2.205	0.00103	0.0023

Rsc = 10KOhm; Csc = 10 nF									
Rs	OP V	OP I	OPPower COA	OP V	OP I	OPPower PSO	OP V	OP I	OPPower GWO
1	2.226	0.00022	0.0005	2.221	0.00022	0.00049	2.218	0.00022	0.00049
50	2.226	0.00022	0.00049	2.221	0.00022	0.00049	2.218	0.00022	0.00049
100	2.227	0.00022	0.00049	2.221	0.00022	0.00049	2.218	0.00022	0.00048
250	2.227	0.00022	0.00048	2.221	0.00022	0.00048	2.218	0.00021	0.00046
500	2.227	0.00021	0.00047	2.221	0.00021	0.00047	2.218	0.0002	0.00045
750	2.227	0.00021	0.00046	2.221	0.00021	0.00046	2.218	0.00019	0.00043
1000	2.227	0.0002	0.00045	2.221	0.0002	0.00045	2.218	0.00019	0.00042

Rsc = 500KOhm; Csc = 10 nF									
Rs	OP V	OP I	OPPower COA	OP V	OP I	OPPower PSO	OP V	OP I	OPPower GWO
1	2.229	4.459E-06	9.9E-06	2.189	4.23E-06	9.27E-06	2.16	3.23E-06	7E-06
50	2.229	4.4580E-06	9.9E-06	2.19	4.22E-06	9.25E-06	2.162	3.22E-06	7E-06
100	2.229	4.4570E-06	9.9E-06	2.198	4.22E-06	9.27E-06	2.165	3.22E-06	7E-06
250	2.229	4.4560E-06	9.9E-06	2.201	4.21E-06	9.26E-06	2.168	3.21E-06	6.9E-06
500	2.229	4.4540E-06	9.9E-06	2.204	4.19E-06	9.24E-06	2.169	3.19E-06	6.9E-06
750	2.229	4.4540E-06	9.9E-06	2.205	4.19E-06	9.23E-06	2.171	3.19E-06	6.9E-06
1000	2.229	4.4540E-06	9.9E-06	2.207	4.19E-06	9.24E-06	2.173	3.18E-06	6.9E-06

Rsc = 1000KOhm; Csc = 10 nF									
Rs	OP V	OP I	OPPower COA	OP V	OP I	OPPower PSO	OP V	OP I	OPPower GWO
1	2.229	2.23E-06	4.97E-06	2.218	2.12E-06	4.70E-06	2.216	1.98E-06	4.39E-06
50	2.229	2.23E-06	4.97E-06	2.218	2.12E-06	4.70E-06	2.216	1.98E-06	4.39E-06
100	2.229	2.23E-06	4.97E-06	2.218	2.12E-06	4.70E-06	2.216	1.98E-06	4.39E-06
250	2.229	2.23E-06	4.97E-06	2.218	2.12E-06	4.70E-06	2.216	1.98E-06	4.39E-06
500	2.229	2.23E-06	4.97E-06	2.218	2.12E-06	4.70E-06	2.216	1.98E-06	4.39E-06
750	2.229	2.23E-06	4.97E-06	2.218	2.12E-06	4.70E-06	2.216	1.98E-06	4.39E-06
1000	2.229	2.23E-06	4.97E-06	2.218	2.12E-06	4.70E-06	2.216	1.98E-06	4.39E-06

Rsc = 1000 Ohm; Csc = 50nF									
Rs	OP V	OP I	OPPower COA	OP V	OP I	OPPower PSO	OP V	OP I	OPPower GWO
1	2.193	0.002191	0.0048	2.189	0.00218	0.0048	2.178	0.00216	0.0047
50	2.195	0.002091	0.0046	2.191	0.00207	0.0045	2.188	0.00205	0.0045
100	2.197	0.001997	0.0044	2.193	0.00198	0.0043	2.19	0.00195	0.0043
250	2.202	0.001761	0.0039	2.196	0.00166	0.0036	2.194	0.00159	0.0035
500	2.207	0.001471	0.0032	2.199	0.00142	0.0031	2.198	0.00138	0.0030
750	2.211	0.001263	0.0028	2.203	0.0012	0.0026	2.203	0.00119	0.0026
1000	2.213	0.001107	0.0024	2.206	0.00107	0.0024	2.205	0.00103	0.0023

Rsc = 1000 Ohm; Csc = 100nF									
Rs	OP V	OP I	OPPower COA	OP V	OP I	OPPower PSO	OP V	OP I	OPPower GWO
1	2.193	0.00219	0.0048	2.189	0.00218	0.0048	2.178	0.00216	0.0047
50	2.195	0.00209	0.0046	2.191	0.00207	0.0045	2.188	0.00205	0.0045
100	2.197	0.002	0.0044	2.193	0.00198	0.0043	2.19	0.00195	0.0043
250	2.202	0.00176	0.0039	2.196	0.00166	0.0036	2.194	0.00159	0.0035
500	2.207	0.00147	0.0032	2.199	0.00142	0.0031	2.198	0.00138	0.0030
750	2.211	0.00126	0.0028	2.203	0.0012	0.0026	2.203	0.00119	0.0026
1000	2.213	0.00111	0.0024	2.206	0.00107	0.0024	2.205	0.00103	0.0023

Simulation results for R_{sc} =1kΩ to 5000kΩ and C_{sc} = 10nF to 100nF

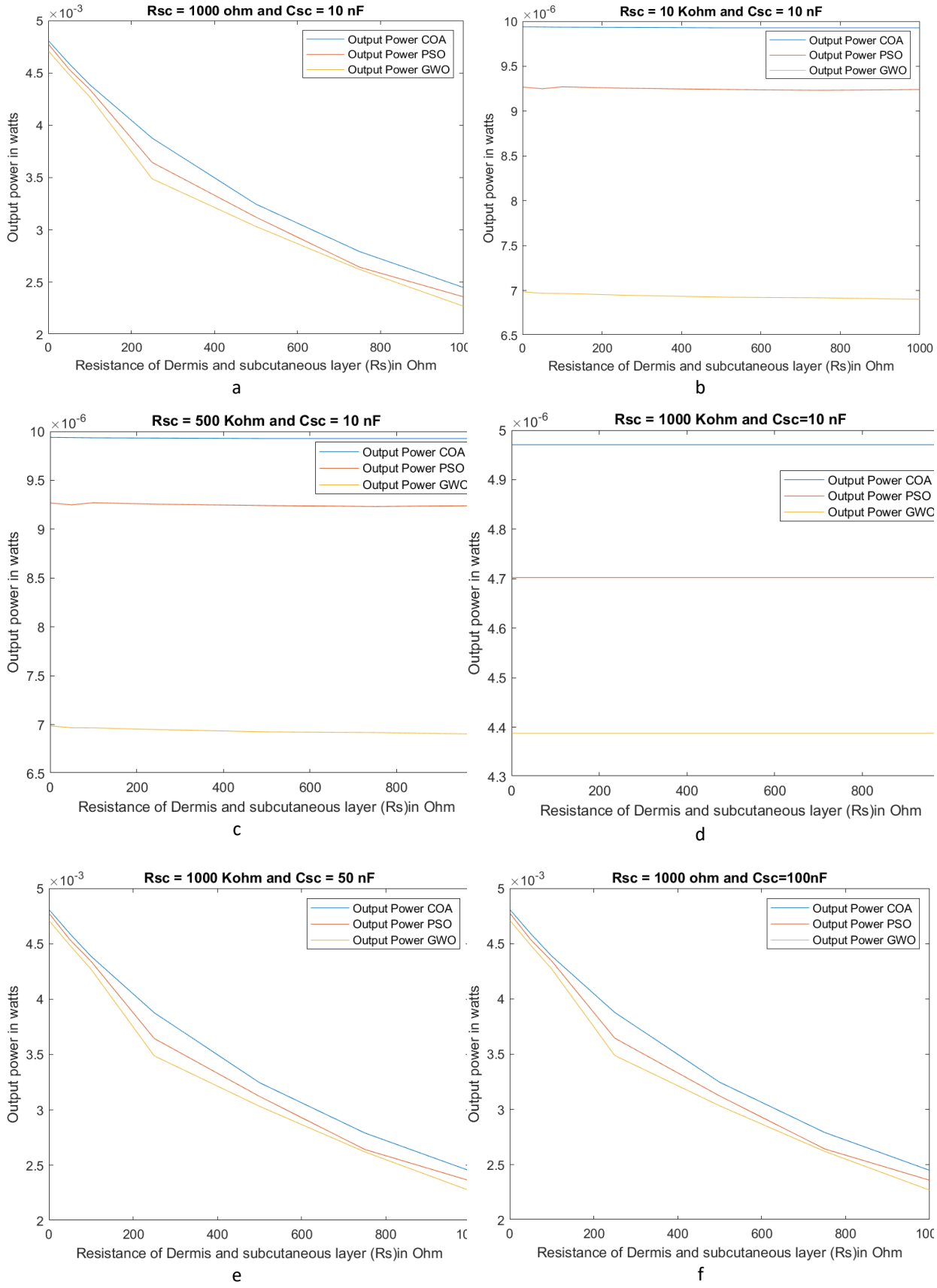

Figure 5 a-f. Plot for various values of R_{sc} and C_{sc}

5. Conclusion

An optimised MPPT controller for equivalent skin model with battery-less cardiac pacemaker is proposed in this project. As PV is utilized to power cardiac pacemaker it is battery less cardiac pacemaker. The PV is connected with the equivalent circuit model. The PV may be affected due to environmental conditions which will be solved by the MPPT controller. The COA is developed to maintain the stability operation by avoiding environmental conditions. Here, the COA is utilized to manage the MPPT controller. The proposed battery-less cardiac pacemaker is designed and executed in MATLAB/Simulink, and performance is evaluated in terms of maximum power, maximum voltage, maximum current, irradiance, the input power of pacemaker, and output power of pacemaker. The projected technique is contrasted with conventional techniques like PSO in addition GWO respectively.

6. References

[1] Xingqun Liang, Sylvia M. Evans, and Yunfu Sun. "Development of the cardiac pacemaker." Cellular and Molecular Life Sciences 74, no. 7 (2017): 1247-1259.

[2] Munna Khan, and Ajai Kumar Singh. "Modeling and simulation of solar boost converter to supply power for cardiac pacemakers." In 2013 IEEE International Symposium on Medical Measurements and Applications (MeMeA), pp. 187-190. IEEE, 2013.

[3] Dominique Méry, and Neeraj Kumar Singh. "Closed-loop modeling of cardiac pacemaker and heart." In International Symposium on Foundations of Health Informatics Engineering and Systems, pp. 151-166. Springer, Berlin, Heidelberg, 2012.

[4] Zhihao Jiang, Miroslav Pajic, Salar Moarref, Rajeev Alur, and Rahul Mangharam. "Modeling and verification of a dual chamber implantable pacemaker." In International Conference on Tools and Algorithms for the Construction and Analysis of Systems, pp. 188-203. Springer, Berlin, Heidelberg, 2012.

[5] Hugo Daniel Macedo, Peter Gorm Larsen, and John Fitzgerald. "Incremental development of a distributed real-time model of a cardiac pacing system using VDM." In International Symposium on Formal Methods, pp. 181-197. Springer, Berlin, Heidelberg, 2008.

[6] Fleur VY Tjong, and Vivek Y. Reddy. "Permanent leadless cardiac pacemaker therapy: a comprehensive review." Circulation 135, no. 15 (2017): 1458-1470.

[7] Geon-Tae Hwang, Hyewon Park, Jeong-Ho Lee, SeKwon Oh, Kwi-Il Park, Myunghwan Byun, Hyelim Park et al. "Self-powered cardiac pacemaker enabled by flexible single crystalline PMN-PT piezoelectric energy harvester." Advanced materials 26, no. 28 (2014): 4880-4887.

[8] Rubens Tofano de Barros, Sebastião Marcos Ribeiro de Carvalho, Marcos Augusto de Moraes Silva, and Juliana Bassalobre Carvalho Borges. "Evaluation of patients' quality of life aspects after cardiac pacemaker implantation." Brazilian Journal of Cardiovascular Surgery 29 (2014): 37-44.

[9] Jyoti Yadav, Asha Rani, and Girisha Garg. "Intelligent heart rate controller for cardiac pacemaker." International Journal of Computer Applications 36, no. 7 (2011): 22-29.

[10] Jongmoon Jang, Pradeep Vallachira Warriam Sasikumar, Fatemeh Navaee, Lorenz Hagelüken, Gurdial Blugan, and Juergen Brugger. "Electrochemical performance of polymer-derived SiOC and SiTiOC ceramic electrodes for artificial cardiac pacemaker applications." Ceramics International 47, no. 6 (2021): 7593-7601.

[11] Yuncong Jiang, Jaber A. Abu Qahouq, and Tim A. Haskew. "Adaptive step size with adaptive-perturbation-frequency digital MPPT controller for a single-sensor photovoltaic solar system." IEEE transactions on power Electronics 28, no. 7 (2012): 3195-3205.

[12] Bhukya Laxman, Anil Annamraju, and Nandiraju Venkata Srikanth. "A grey wolf optimized fuzzy logic based MPPT for shaded solar photovoltaic systems in microgrids." International Journal of Hydrogen Energy 46, no. 18 (2021): 10653-10665.

[13] Hai Tao, Mehrdad Ghahremani, Faraedoon Waly Ahmed, Wang Jing, Muhammad Shahzad

Nazir, and Kentaro Ohshima. "A novel MPPT controller in PV systems with hybrid whale optimization-PS algorithm based ANFIS under different conditions." Control Engineering Practice 112 (2021): 104809.

[14] Mohammad Junaid and Khan. "A Novel Hybrid Maximum Power Point Tracking Controller Based on Artificial Intelligence for Solar Photovoltaic System Under Variable Environmental Conditions." Journal of Electrical Engineering & Technology (2021): 1-11.

[15] Ali M Eltamaly, M. S. Al-Saud, Ahmed G. Abokhalil, and Hassan MH Farh. "Simulation and experimental validation of fast adaptive particle swarm optimization strategy for photovoltaic global peak tracker under dynamic partial shading." Renewable and Sustainable Energy Reviews 124 (2020): 109719.

[16] Sara Azimi, Allahyar Golabchi, Abdolhossein Nekookar, Shahram Rabbani, Morteza Hassanpour Amiri, Kamal Asadi, and Mohammad Mahdi Abolhasani. "Self-powered cardiac pacemaker by piezoelectric polymer nanogenerator implant." Nano Energy 83 (2021): 105781.

[17] Chunhua Liu, Chaoqiang Jiang, Jingjing Song, and K. T. Chau. "An effective sandwiched wireless power transfer system for charging implantable cardiac pacemaker." IEEE Transactions on Industrial Electronics 66, no. 5 (2018): 4108-4117.

[18] Adnan Mukhtar, and Farhan Mukhtar. "Adaptive Fractional Order PID Controller Design of a Pacemaker based on Heart Rate Control Strategy." International Research Journal of Engineering and Technology (IRJET) (2020): 1681-1685.

[19] Munna Khan, Ajai Kumar Singh, and Syed Shakir Iqbal. "SPICE simulation of implantable solar power supply for sustainable operation of cardiac biosensors." International Journal of Biomedical Engineering and Technology 18, no. 2 (2015): 168-185.

[20] Andreas Haeberlin, Adrian Zurbuchen, Sébastien Walpen, Jakob Schaerer, Thomas Niederhauser, Christoph Huber, Hildegard Tanner et al. "The first batteryless, solar-powered cardiac pacemaker." Heart rhythm 12, no. 6 (2015): 1317-1323.

[21] Ayan Banik, Anurag Shrivastava, Ravindra Manohar Potdar, Sanjiv Kumar Jain, Santosh Gopal Nagpure, and Mukesh Soni. "Design, Modelling, and Analysis of Novel Solar PV System using MATLAB." Materials Today: Proceedings (2021).

[22] Mustafa Sinasi Ayas, and Erdinc Sahin. "FOPID controller with fractional filter for an automatic voltage regulator." Computers & Electrical Engineering 90 (2021): 106895.

[23] Ayşen Demirören, Serdar Ekinci, Baran Hekimoğlu, and Davut Izci. "Opposition-based artificial electric field algorithm and its application to FOPID controller design for unstable magnetic ball suspension system." Engineering Science and Technology, an International Journal 24, no. 2 (2021): 469-479.

[24] M.Khishe, and Mohammad Reza Mosavi. "Chimp optimization algorithm." Expert systems with applications 149 (2020): 113338.

[25] M.Khishe, and M. R. Mosavi. "Classification of underwater acoustical dataset using neural network trained by chimp optimization algorithm." Applied Acoustics 157 (2020): 107005.

[26] Nikola Pe˘rinka, Matija Štrbac, Milos Kosti´c, Jovana Maleševi´c, Nélson Castro,* Vítor Correia, and Senentxu Lanceros-Méndez. “Design and Fabrication of Printed Human Skin Model Equivalent Circuit: A Tool for Testing Biomedical Electrodes without Human Trials” Adv. Eng. Mater. 2022, 24, 2100684

[27] Dhruba Jyoti Bora and Rajdeep Dasgupta, Estimation of skin impedance models with experimental data and a proposed model for human skin impedance IET Syst Biol. 2020 Jun; 14(3): 147–159.